

# Study on SiN<sub>x</sub> passivated Cu/Ta/SiO<sub>2</sub>/Si multilayer structure

K. M. LATT\*, H. S. PARK

*School of Materials Engineering, Nanyang Technological University,  
Nanyang Avenue, Singapore 639798  
E-mail: p101282@ntu.edu.sg*

H. L. SENG, T. OSIPOWICZ

*Department of Physics, National University of Singapore, Faculty of Science,  
Lower Kent Ridge Road, Singapore 119260*

Y. K. LEE

*School of Materials Engineering, Nanyang Technological University,  
Nanyang Avenue, Singapore 639798*

Silicon nitride (SiN<sub>x</sub>) thin film layers were deposited on Cu/Ta/SiO<sub>2</sub>/Si multilayer structures by Plasma Enhanced Chemical Vapor Deposition at the temperature 285°C. The influence of post deposition thermal annealing treatments on the micro-structural, compositional and thermal stability study of SiN<sub>x</sub>/Cu/Ta/SiO<sub>2</sub>/Si multilayer structure was studied and compared with unpassivated, Cu/Ta/SiO<sub>2</sub>/Si multilayer structure. It was found that after SiN<sub>x</sub> passivation, the formation of Cu<sub>2</sub>O and Ta<sub>2</sub>O<sub>5</sub> was significantly reduced and the structure becomes more stable than unpassivated one. The reaction between Cu, Ta and O was not found in this SiN<sub>x</sub>/Cu/Ta/SiO<sub>2</sub>/Si multilayer structure but the out diffusion of Ta to the Cu surface was unable to be suppressed. The Ta barrier was observed to fail at temperatures above 750°C due to the formation of Ta<sub>x</sub>N<sub>y</sub>, at the interface of SiN<sub>x</sub>/Cu.

© 2002 Kluwer Academic Publishers

## 1. Introduction

Currently there is a large effort to develop a process with which to utilize copper in place of aluminum as a conductor in microelectronic circuits. However, there are a number of issues, which need to be addressed [1–4] before such a substitution can take place. One of these is that copper oxidation is not self-limiting, and therefore some method of passivating the surface of copper is needed. A second group of concerns relates to the copper-dielectric interface. Adhesion at this surface needs to be good, and this interface must act as a diffusion barrier to the transport of copper ions from the metal into sensitive regions of the devices. These characteristics are compounded for integration with a high temperature (>400°C) metallization process. A number of approaches have been investigated for passivation of the exposed surface of Cu including ion implantation, formation of surface silicides, treatment with organic inhibitors, annealing bilayer [4, 5–7] and doping the copper with the metals which can be used to passivate the surface of the copper [4, 8–10]. Dielectric passivation films may be more favorable to suppress Cu oxidation because the process using dielectric passivation is easier. Thin films of silicon nitride have been extensively used in various technological areas,

especially in the fabrication of microelectronic devices as oxidation masks, gate dielectric, interlevel insulators, and final passivation layers. All these applications are due to silicon nitride's remarkable properties such as high thermal stability, chemical inertness, extreme hardness, and good dielectric properties. In this work, we have used SiN<sub>x</sub> as a passivation layer to protect from the oxidation of Cu metallization.

The usual approach to deal with the second problem is the deposition of a diffusion barrier/adhesion promoter layer between the dielectric materials and the copper. Many possible thin film materials have been explored varying from low melting point metals, [1, 11, 12] to refractory metals [4, 13] to amorphous carbon [14]. In order to find a suitable diffusion barrier, a significant amount of research work has been performed, and various diffusion barriers, including refractory metal (Ta and W) [15, 16] nitrides (TiN and TaN) [17, 18] and compounds (TiW and Ta-Si-N) [19, 20] have been proposed. Among the proposed diffusion barriers, Ta has been widely investigated as a single metal diffusion barrier for Cu metallization because it not only has a high melting point (2996°C) and silicidation temperature (~650°C), but it also shows a very low solubility in Cu [21]. In this communication we report

\*Author to whom all correspondence should be addressed.

the effect of a thin passivation layer of PECVD-SiN<sub>x</sub> on top of Cu in the Cu/Ta/SiO<sub>2</sub>/Si multilayer structure and subsequent annealing.

## 2. Experimental details

For all sample preparation and experiments described in this study used 8" Si (100) wafers. Si wafers were cleaned in 10 : 1 diluted HF solution and rinsed in deionized water before SiO<sub>2</sub> deposition. First, a 500 nm thick plasma enhanced chemical vapor deposited (PECVD) SiO<sub>2</sub> dielectric was deposited by using a gas mixture of SiH<sub>4</sub>, O<sub>2</sub> and Ar at 350°C on 8" Si wafers. The SiO<sub>2</sub> deposited Si substrates were loaded into the IMP sputtering chamber for the deposition of Ta (30 nm) and subsequently Cu (200 nm) without breaking the vacuum. The IMP deposition process has been described in detail elsewhere [22]. Then, the 20 nm thick passivation film, SiN<sub>x</sub>, was deposited from a silane (SiH<sub>4</sub>) and ammonia (NH<sub>3</sub>) mixture at 285°C by Plasma Enhanced Chemical Vapor Deposition (PECVD) system. This technology provides low substrate temperature and allows its use in temperature sensitive materials. Also, it has advantages of low cost and small area occupation. The properties of film made by PECVD are influenced by deposition parameters and can be tailored to the requirement over a wide range. The PECVD deposition process has been described in detail elsewhere [23]. The samples were annealed for 35 min in N<sub>2</sub> ambient up to 850°C from 350°C with 100°C intervals. X-ray diffraction was used for the analysis of reaction product phases and the interdiffusion of the elements across the interface, respectively. X-ray diffraction (XRD), scanning electron microscopy (SEM) and Rutherford backscattering spectrometry (RBS) were employed in conjunction with electrical measurements to examine the failure mechanism.

## 3. Results and discussion

The X-ray diffraction (XRD) measurements were performed with a RIGAKU model RINT2000 diffractome-

ter using a  $\gamma = 2.5^\circ$  grazing incident angle geometry. The Cu K<sub>α</sub> X-ray ( $\lambda = 1.542 \text{ \AA}$ ) detection was done from  $2\theta = 20^\circ$  to  $2\theta = 85^\circ$  with scan speed of 4°/min and scan step 0.05° for the analysis of reaction product phases and the interdiffusion of the elements across the interface, respectively. Fig. 1 shows the XRD pattern obtained from the as-deposited samples of SiN<sub>x</sub> coated Cu/Ta/SiO<sub>2</sub>/Si multilayer structure. As see in Fig. 1 the reflection lines from SiN<sub>x</sub> and Ta are broad in shape and weak in intensity, while that from Cu are sharp and strong as compare with that of from SiN<sub>x</sub> and Ta. Pure Ta sputtered in pure Ar ambient on SiO<sub>2</sub> grown as the high-resistivity (200 μΩ-cm) tetragonal metastable phase and apparently polycrystalline. The XRD pattern (inset) reveals that the peaks centered approximately at 33.55°, 38.2° and 43.30° were correspond to those of tetragonal β-Ta and were indexed to the (002), (202) and (413) respectively [24]. The Cu film sputter deposited on Ta diffusion barrier has a strong (111) preferred orientation at 2θ angle of 43.30° but low intensity peaks of (200) and (220) were also observed at 50.43° and 74.13°. Fig. 1 reveals the broad low intensity reflection lines centered at 2θ angles of 13.439° and 33.153° can be indexed as β-Si<sub>3</sub>N<sub>4</sub> (100) and (101) [24] showing crystalline structure since there is a report on microstructure of SiN<sub>x</sub> which depends on the deposition temperature. According to their results, the transformation from amorphous to crystalline structure for SiN<sub>x</sub> films occurs for the deposited temperatures in the range of 200–250°C [25].

The surface morphologies and grain sizes of the as-deposited Ta diffusion barrier, Cu metallization layer and SiN<sub>x</sub> passivation layer were examined by atomic force microscopy. AFM was performed using a Nanoscope III multimode atomic force microscope. Data were collected in tapping mode AFM with silicon cantilevers at resonance frequencies in the range of 200–300 KHz. It is important to know the microstructure of the IMP-Ta diffusion barrier because they play an important role on the texture of the to be deposited

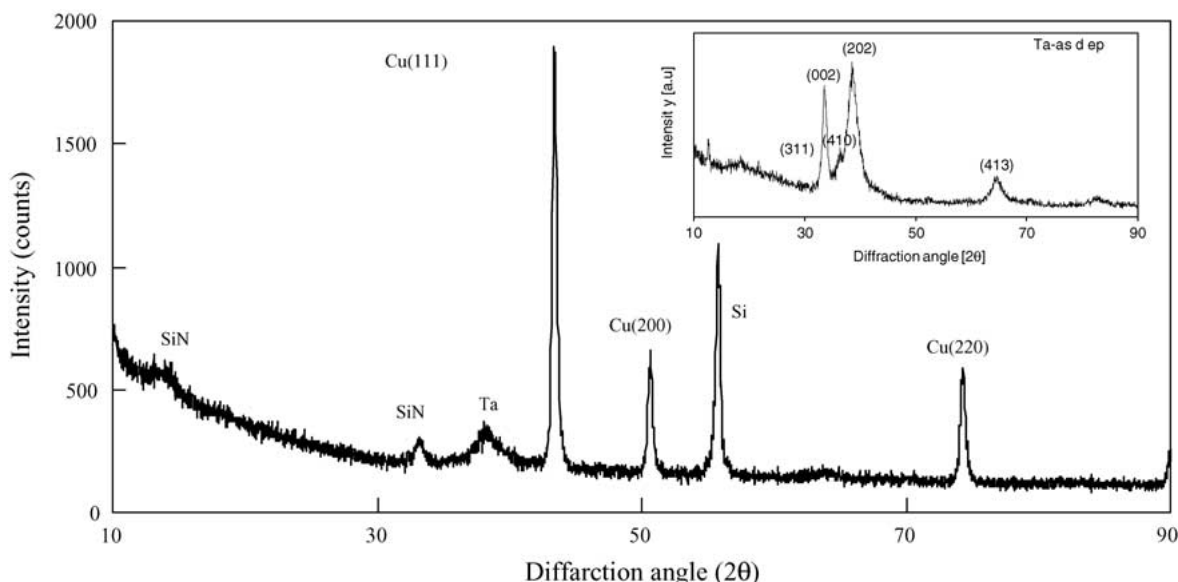


Figure 1 XRD pattern obtained from the as deposited samples of Si<sub>3</sub>N<sub>4</sub> coated Cu/Ta/SiO<sub>2</sub>/Si multilayer structure and the XRD pattern for as-deposited tantalum showing β-Ta (inset).

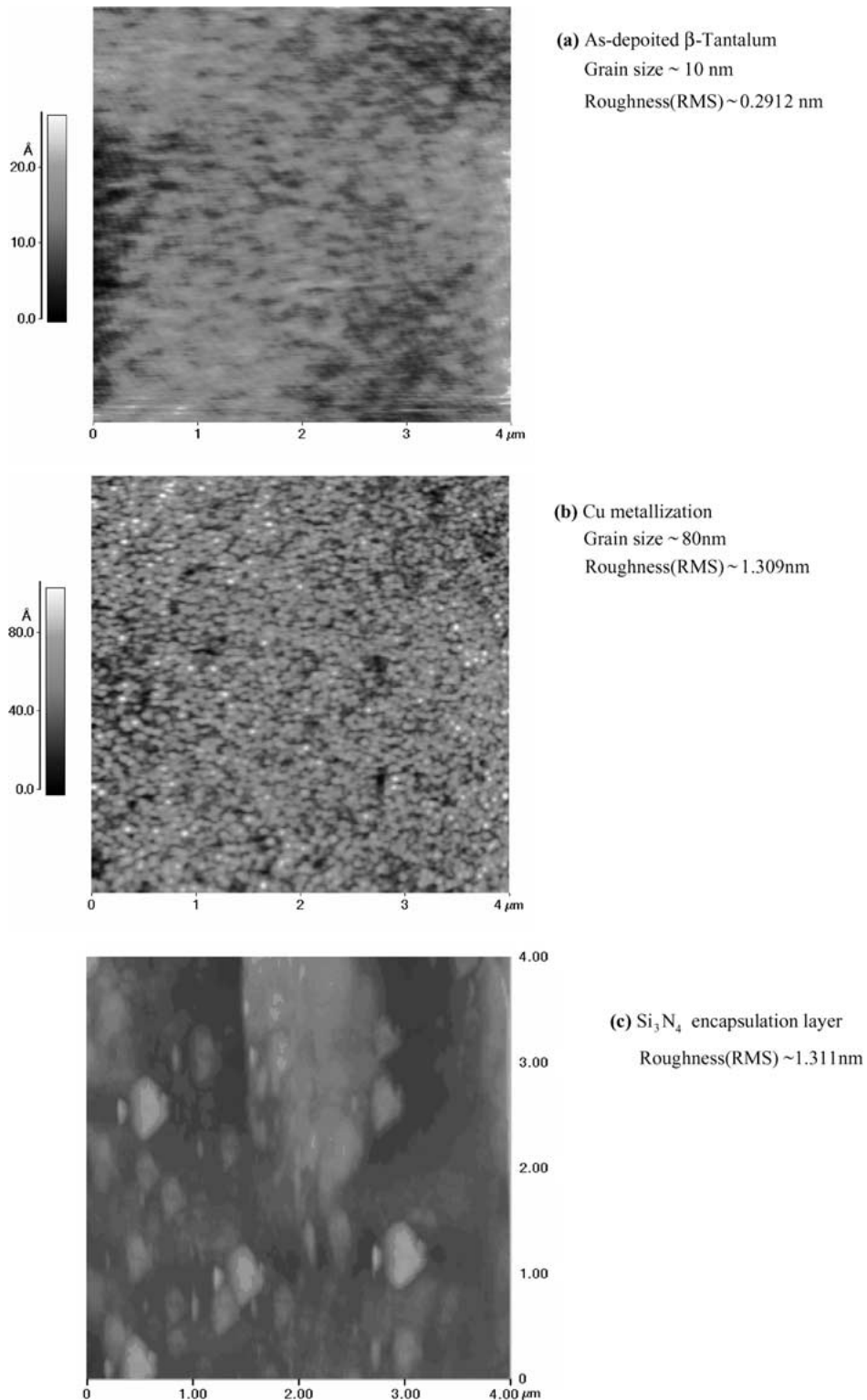


Figure 2 AFM measurement result for SiN coated Cu/Ta/SiO<sub>2</sub>/Si multilayer structures before deposition of the next subsequent layer (a)  $\beta$ -Tantalum (b) Cu metallization and (c) the Si<sub>3</sub>N<sub>4</sub> encapsulation layer deposited on Cu.

films. AFM measurements demonstrate a smooth and nonporous surface morphology with a surface roughness (rms) of  $\sim 0.2912$  nm for a 30 nm Ta Film, documented by the AFM surface plot of Fig. 2a, which consists of very fine grains with a mean grain size of  $\sim 10$  nm. The crystalline Cu sample exhibits small bumps with grain size of about  $\sim 80$  nm and a roughness of  $\sim 1.309$  nm as shown in Fig. 2b. These bumps may correspond to the columnar structure of the film. The dielectric SiN<sub>x</sub> layer, which deposited on Cu (111)

with the ratio of SiH<sub>4</sub>/NH<sub>3</sub> = 1 has a roughness of  $\sim 1.311$  nm Fig. 2c. The surface morphology of the silicon nitride film is grown in island mode and composed of very fine particles.

Before describing our results of thermal stability of the SiN<sub>x</sub> passivated Cu/Ta/SiO<sub>2</sub>/Si multilayer structures, it may be worthwhile to present the results and the solid-phase reactions in the unpassivated Cu(200 nm)/Ta(30 nm)/SiO<sub>2</sub>/Si multilayer structure [26]. The graphs presented in Fig. 3 indicate the change

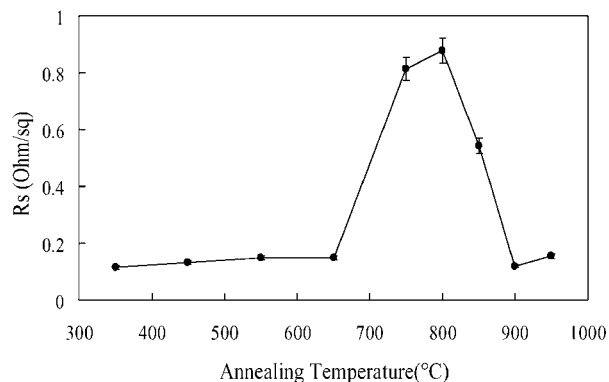


Figure 3 Sheet resistance of Cu/Ta/SiO<sub>2</sub>/Si multilayer structure as a function of annealing temperature.

in sheet resistance measured on the Cu/Ta/SiO<sub>2</sub>/Si structure as a function of annealing temperature in N<sub>2</sub> ambient for 35 min. The measured sheet resistance values were dominated by the copper thin film since the copper film (200 nm and 1.72 μΩ-cm) is much thicker and has a markedly lower resistivity than Ta film (30 nm and 200 μΩ-cm) and any reaction products. Since the top Cu layer of 200 nm carries nearly all the current, the sheet resistance measurements monitor the condition and the quality of the Cu overlayer. Hence, these curves

can be used to estimate the degree of intermixing, reaction, and changes of integrity across the metallization layers as well. According to this figure, all samples, annealed up to 650°C can maintain the same level of sheet resistance as the as-deposited samples. The abrupt rise in sheet resistance after 650°C for Cu/Ta/SiO<sub>2</sub>/Si structure is primarily attributed a partial intermixing between Cu and the underlying films and/or a symptom of a catastrophic failure caused by an overall reaction involving all the metallization layers. The sheet resistance of the Cu/Ta/SiO<sub>2</sub>/Si structure drop back to a very low value after 800°C annealing which is probably due to the β-Ta (tetragonal) to α-Ta (body centered cubic) phase transformation since β-Ta has a resistivity of 200 μΩ-cm and α-Ta phase has a relatively low value, 15 μΩ-cm [27, 28].

Rutherford Back Scattering (RBS) was used to examine reaction and interdiffusion between the Cu metallization layer and a Ta diffusion barrier. Rutherford backscattering spectrometry (RBS) spectra were taken with 2 MeV He<sup>+</sup> ions at a scattering angle of 160° using a 50 mm<sup>2</sup> Passivated Implanted Planar Silicon (PIPS) detector of 13.5 KeV resolution. Fig. 4 shows the RBS depth profile of the Cu/Ta/SiO<sub>2</sub>/Si sample annealed for 35 min at various temperatures in N<sub>2</sub> ambient. The surface scattering energies for O, Si, Cu and Ta are indicated. The as-deposited films exhibit two inseparable

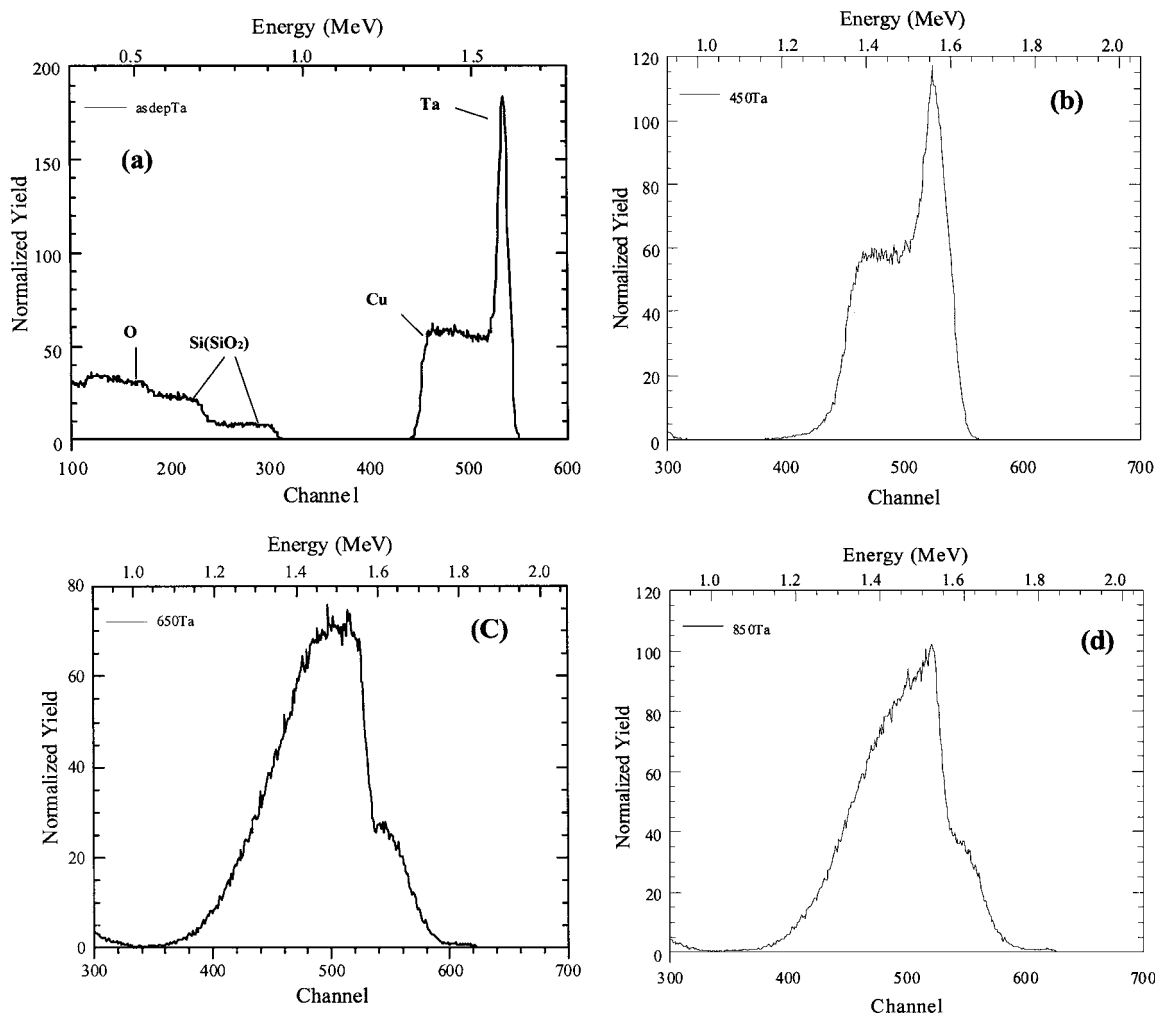


Figure 4 2 MeV He<sup>+</sup> RBS spectra of the Cu/Ta/SiO<sub>2</sub>/Si multilayer structure annealed at various temperatures for 35 min in N<sub>2</sub> ambient (a) as deposited (b) 450°C (c) 650°C (d) 850°C.

Ta and Cu peaks without evidence of intermixing. The Ta layer appears to remain largely intact up to 450°C. For the sample annealed at 550°C, the motion of Ta atoms toward the Cu surface gradually begun, but the integrity of the structure is still remained. For the sample annealed at 650°C (Fig. 4c), the motion of elements are more clearly observed and the RBS spectra show that the gradient of the trailing edge of the Cu signal changes and a small amount of Ta appears at the higher energy levels. Out-diffusion of Ta into the Cu films seems to start along the grain boundaries, due to the columnar structure of Cu film, in the range of ~550 to 600°C. However, the sheet resistance of the structure remains unchanged if the annealing temperature does not exceed 650°C. The following features were also observed for samples annealing temperature higher than 650°C (i) a significant reduction of the Ta peak height and the broadening of the Ta peak (ii) the tailing of Cu peak into even lower energy. These features indicate a possible formation of a new (Cu-Ta) compound and XRD result confirmed the formation of  $\text{Cu}_x\text{Ta}_y\text{O}_z$  [26]. When the annealing temperature reaches 850°C (Fig. 4d), a new Ta peak appears at the energy level of 1.836 MeV and grows indicating that Ta had migrated to the surface, giving a peak in the RBS signal at the surface energy expected for Ta. Annealing to higher temperatures resulted in accumulation of Ta on the surface of Cu film. The back edge of the Cu signal becomes more graded with increasing temperature, implying that Cu film starts to agglomerate, thus exposing part of the Ta film to the ambient. As the results of RBS are greatly affected by the morphologies and interface roughness of the samples, they were interpreted in conjunction with SEM observation.

The surface morphologies of the Cu/Ta/SiO<sub>2</sub>/Si multilayer structure was examined by the JEOL 5410 scanning electron microscopy operated at 20 KV. Fig. 5a shows surface morphology of the samples before annealing; it is evident that a smooth and uniform surface was observed. A similar morphology was also found for samples annealed at temperatures less than 500°C. At 650°C, motion of Ta atoms towards the Cu surface was initiated with high grain concentration was observed on the surface (Fig. 5b). The surface become rougher, but does not seem to have any voids. This is supported by the RBS spectrum of the sample annealed at this temperature (Fig. 4c) and sudden increase in sheet resistance value (Fig. 3). The average grain size at this temperature was about 1 μm. At the temperature of 850°C (Fig. 5), the surface of Cu/Ta/SiO<sub>2</sub>/Si multilayer structure shows an increase in average grain size, and agglomeration of Cu film, that exposed the underneath Ta layer to the ambient, was clearly observed. The SEM figures clearly reveal, even in low magnification, the patches after high temperature annealing. The grazing incident angle of 2.5° identified the intermixing and new phase formation for the SiN<sub>x</sub>/Cu/Ta/SiO<sub>2</sub>/Si structure annealed up to 850°C. As shown in Fig. 6 there is a distinction in XRD spectra between samples annealed below and above 750°C. Annealing temperatures lower than 750°C, only a strong pure Cu (111) peak was found in the spectrum at 2θ angle of 43.3°

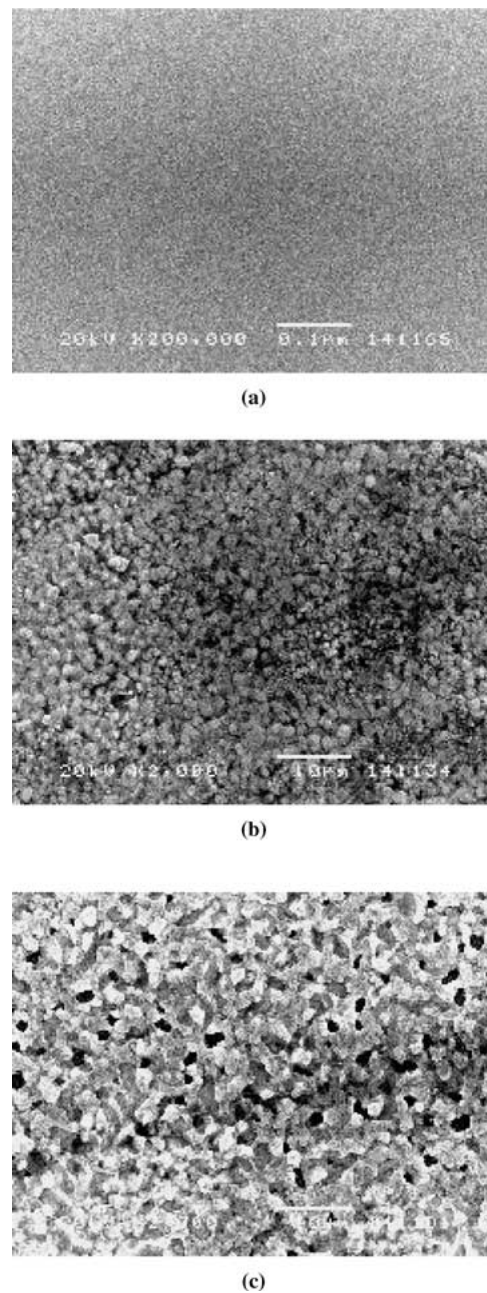


Figure 5 SEM images of Cu/Ta/SiO<sub>2</sub>/Si multilayer structure before (a) and after annealing at (b) 650°C and (c) 850°C for 35 min in N<sub>2</sub> ambient.

[24]. Any reaction involving Cu, Ta, O or Si was not observed. Distinctly, at 750°C, several new peaks were found which were identified as Ta<sub>6</sub>O (001) at 2θ° angles of 38.80, and Ta<sub>2</sub>N (111) at 38.90° [24] respectively and the β-Ta peak was overlap with those new peaks. It is clear that Ta was reacted N<sub>2</sub> which dissociated, probably, form the SiN<sub>x</sub> layer and formed Ta<sub>x</sub>N<sub>y</sub> since it was reported that SiN<sub>x</sub> have Si and N dangling bonds as the defects and the defect density was increased for higher annealing temperature [29]. After annealing at 750°C, a new low intensity peaks were appeared at 2θ angle of 20.680° which was identity as α-Si<sub>3</sub>N<sub>4</sub> (101) and more peaks were observed at 38.535° and 36.53° which can be indexed as α-Si<sub>3</sub>N<sub>4</sub> (102) and (220) [23]. This reveal the fact that β-Si<sub>3</sub>N<sub>4</sub> has undergone a transformation into α-Si<sub>3</sub>N<sub>4</sub> when annealing temperature higher than 750°C since β-Si<sub>3</sub>N<sub>4</sub> was totally disappeared from the

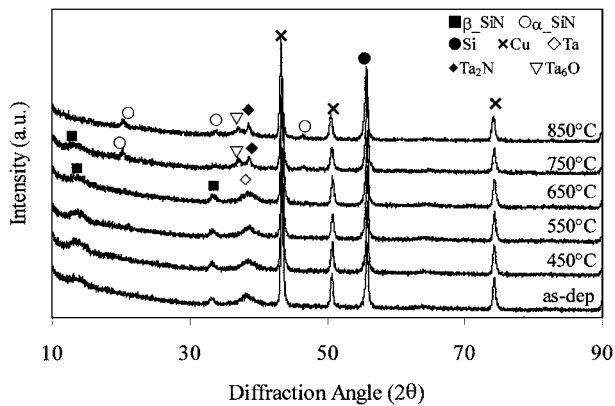


Figure 6 XRD measurement results of  $\text{SiN}_x/\text{Cu}/\text{Ta}/\text{SiO}_2/\text{Si}$  multilayer structure before and after annealing at various temperatures for 35 min in  $\text{N}_2$  ambient.

XRD spectrum. However, no significant changes in Cu peaks were observed through out annealing process.

For the case of the presence of an oxide,  $\text{Ta}_6\text{O}$ , at annealing temperature at  $750^\circ\text{C}$ , since Ta has very affinity to oxygen, it forms one stable oxide  $\text{Ta}_2\text{O}_5$  together with several metalstable oxides. In an unpassivated structure [26], it was found that  $\text{Ta}_2\text{O}_5$  was formed after annealing at  $650^\circ\text{C}$  due to the oxygen mainly incorporated during the deposition process in the  $\text{Cu}/\text{Ta}/\text{SiO}_2/\text{Si}$  mul-

tilayer structure. After passivated with  $\text{SiN}_x$ , it was observed that only  $\text{Ta}_6\text{O}$  was formed instead of the  $\text{Ta}_2\text{O}_5$ . In addition, the solubility of oxygen in the body-centre-cubic (bcc) lattice of Ta is high ( $\sim 5\text{at.}\%$  at  $1500^\circ\text{C}$ ) [30]. The presence of oxygen in the Ta layers is indicated indirectly by the formation of metalstable  $\beta$ -Ta phase, which is a body centered cubic (bcc)-based super lattice structure with only slight tetragonal distortion. The incorporation of oxygen of more than 2–3 at.% in the Ta layer at the annealing temperatures used in the study leads to the formation of metalstable oxide,  $\text{Ta}_6\text{O}$ . The solubility of oxygen in the metalstable  $\beta$ -Ta is not known accurately but it has to be larger than that of stable  $\alpha$ -Ta. The larger solubility of oxygen into the  $\beta$ -Ta layer is expected to rule out the possibility that the segregation of oxygen in the grain boundaries of the Ta film inhibits Cu diffusion.

To examine reaction and interdiffusion between the Cu meatllization and Ta diffusion barrier layer at different temperatures, Rutherford backscattering spectrometry was used (Fig. 7). The discrete layers of Ta and Cu are clearly seen in the spectrum from the samples without annealing. The measurement shows that these layers were present up to  $650^\circ\text{C}$ . At  $750^\circ\text{C}$  there is a shift in Ta peak towards the surface, but it can be attributed to the thickness variations in the Cu layer as the trailing edge of the Cu peak also shifts about the same

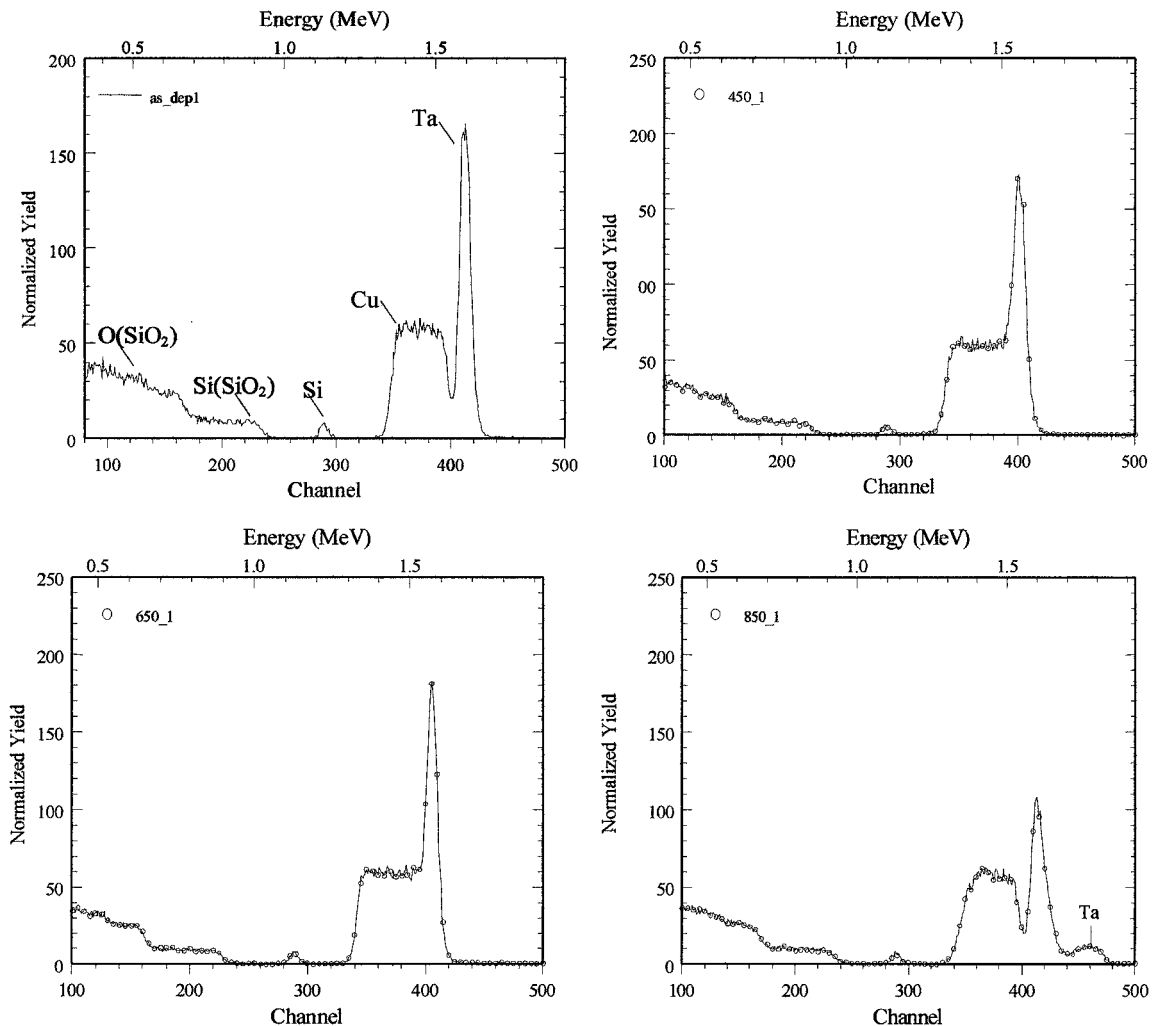


Figure 7 2 MeV  $\text{He}^+$  RBS spectra of the  $\text{Cu}/\text{Ta}/\text{SiO}_2/\text{Si}$  multilayer structure annealed at various temperatures for 35 min in  $\text{N}_2$  ambient.

amount. The occurrence of the small surface peak corresponding to that of Ta indicates that a small amount of Ta has diffused to the surface of Cu. The motion of Ta to the surface of Cu is unaffected by the  $\text{SiN}_x$  capping layer. The first event of the reaction sequence is the accumulation of Ta at the  $\text{Cu/SiN}_x$  interface at  $750^\circ\text{C}$  annealing which causes reactions between Ta and  $\text{SiN}_x$  passivation layer and produced  $\text{Ta}_x\text{N}_y$  after annealing at  $750^\circ\text{C}$ . However, the interface between Ta and  $\text{SiO}_2$  remains smooth and intact at this temperature. For the samples annealed at  $850^\circ\text{C}$  (Fig. 7d), the motion of Ta atoms toward the Cu surface layer are more clearly observed but in-diffusion of Cu atoms as well as partial diffusion of Ta into  $\text{Si/SiO}_2$  were not found. According to the RBS analysis, it is believed that tantalum nitride could be formed on the Cu surface at this temperature under this experimental condition. Concerning the TaN formation, the following features were observed at  $850^\circ\text{C}$  (i) a considerable motion of Ta atoms toward the surface, (ii) a reduction of the Ta signal height as compared with the as deposited samples (iii) the Ta signal gets broader. These features are indicative of the reaction between Ta and N and formation of TaN at the interface of  $\text{SiN}_x/\text{Cu}$ , which is consistent with the XRD result.

Fig. 8 shows the surface morphologies of  $\text{SiN}_x/\text{Cu}/\text{Ta}/\text{SiO}_2/\text{Si}$  multilayer structure annealed at various temperatures in  $\text{N}_2$  ambient for 35 min. Fig. 8a shows the surface morphology of  $\text{SiN}_x$  surface before annealing which reveals a smooth and uniform surface. A similar morphology was also found but some ridges appeared for sample annealed at temperature of  $650^\circ\text{C}$ . SEM micrograph at  $850^\circ\text{C}$  (Fig. 8c) shows that the  $\text{SiN}_x$  surface exhibit changes as compare to that of at  $650^\circ\text{C}$ , ridges and patches were seen more clearly and grew with the increasing temperature. However, as compare to the uncoated  $\text{Cu}/\text{Ta}/\text{SiO}_2/\text{Si}$  structure, the  $\text{SiN}_x$  passivated structure has become more stable in thermal treatment and shows less out diffusion of Ta atoms to the Cu surface and interfacial reactions at  $\text{Cu}/\text{Ta}$  interface. Evidences of agglomeration of Cu were not observed in the RBS analysis of  $\text{SiN}_x/\text{Cu}/\text{Ta}/\text{SiO}_2/\text{Si}$  multilayer structure even at  $850^\circ\text{C}$ . Both structures did not show any evidence (formation of  $\text{Cu}_x\text{Si}_y$ ,  $\text{Ta}_x\text{Si}_y$ ) of Cu diffusion through Ta diffusion barrier but exhibit the out-diffusion of Ta to the Cu surface. The out-diffusion of Ta can be explained by two ways (i) according to AFM measurement, the Cu has the average grain size of  $\sim 80$  nm while Ta has a much smaller grain size, of the order of  $\sim 10$  nm, so it is easier for Ta atoms to migrate to Cu film rather than Cu atoms to Ta film despite the faster lattice diffusion of Cu compared with Ta, and it is not necessary for Cu to diffuse first at the interface; (ii) it is still possible for Ta to diffuse outwards, due to the high affinity toward oxygen, if there is enough oxygen available in the ambient. It is thought that Ta has the main moving elements during TaN formation at the interface of  $\text{SiN}_x/\text{Cu}$  and Cu just offered short-circuit diffusion paths for Ta to react with N atoms which were dissociated from  $\text{SiN}_x$ . Apart from this the formation of tantalum oxides ( $\text{Ta}_x\text{O}_y$ ) can be assumed as another reason for the retarded diffusion of the Cu

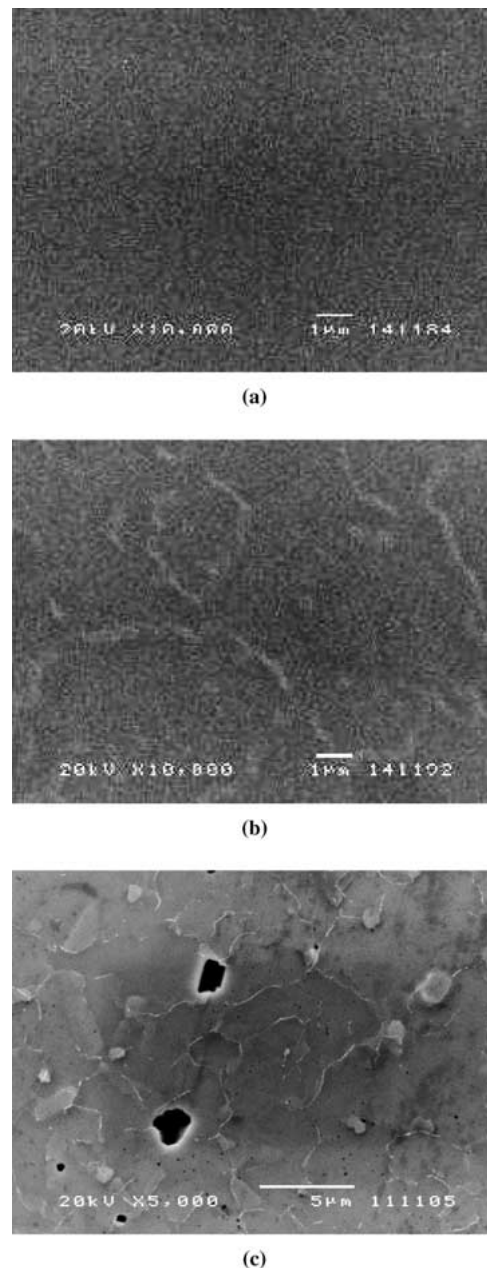


Figure 8 SEM images of  $\text{Si}_3\text{N}_4$  on top of  $\text{Cu}/\text{Ta}/\text{SiO}_2/\text{Si}$  multilayer structure before (a) and after annealing at (b)  $650^\circ\text{C}$  and (c)  $850^\circ\text{C}$  for 35 min in  $\text{N}_2$  ambient.

atoms. Below  $650^\circ\text{C}$ , in the XRD analysis (Fig. 6), the presence of the tantalum oxide layer prevents the diffusion of Cu atoms through Ta film into the  $\text{SiO}_2/\text{Si}$  layer. It was reported that the driving force for the dissolution of oxygen into the Ta layer is very high [30]. Hence, the Ta-O solid solution is expected to be more stable than the oxide layer ( $\text{Ta}_2\text{O}_5$ ) in a large temperature range. However, the dissolution of oxygen into the Ta-rich layer becomes possible only after the relaxation of kinetic constraints. This will take place when the intrinsic diffusion coefficient of oxygen in the Ta layer is high enough. Since the intrinsic diffusion coefficients are exponentially dependent on temperature, the kinetics of the dissolution reaction change strongly with temperature. Thus, it was suggested that at temperature below  $650^\circ\text{C}$  kinetic constraints prevent the dissolution of the oxide layer which is impeding the migration of Cu atoms. As a result, no evidences of

silicides formation like  $\text{Cu}_x\text{Si}_y$  and  $\text{Ta}_x\text{Si}_y$  was seen in the XRD and RBS results in this new structure. On the other hand, in our previous work it was found that the severe reactions were taking place between Cu,  $\text{Cu}_2\text{O}$ , Ta and  $\text{Ta}_2\text{O}_5$  and produced  $\text{Cu}_x\text{Ta}_y\text{O}_z$  after annealing at  $750^\circ\text{C}$ . These kind of reaction products were not appeared after passivation layer was deposited on Cu and oxidation of Cu metallization layer was protected effectively with this dielectric passivation layer. The mechanisms of the Cu films oxidation at low temperatures were studied by Li *et al.* [31]. It was observed that Cu is first oxidized to  $\text{Cu}_2\text{O}$  at the temperature as low as  $200^\circ\text{C}$  and then to  $\text{CuO}$  at  $300^\circ\text{C}$ . The oxidation starts at the surface and progresses slowly into the bulk. Since the inward diffusion of oxygen proceeds gradually as a function of annealing time, the complete oxidation from  $\text{Cu}_2\text{O}$  to  $\text{CuO}$  depends on the annealing condition. In the previous experiment, the observed microstructure of the sample annealed at  $650^\circ\text{C}$  (Fig. 5b) is likely the result of partial formation of  $\text{Cu}_2\text{O}$ . XRD results revealed the formation of  $\text{Cu}_2\text{O}$  after annealing at  $750^\circ\text{C}$  and grown as the temperature increased. It might be due to the  $\text{N}_2$  ambient annealing, no transformation of  $\text{Cu}_2\text{O}$  to  $\text{CuO}$  was seen in XRD analysis. However, the formation Cu oxide was existed in  $\text{Cu}/\text{TaN}/\text{SiO}_2/\text{Si}$  multilayer structure due to annealing process but any form of Cu oxidation was not observed in  $\text{SiN}_x$  passivated  $\text{Cu}/\text{TaN}/\text{SiO}_2/\text{Si}$  multilayer structure throughout the annealing process.

#### 4. Conclusions

The effect of passivation layer of  $\text{SiN}_x$  on the thermal stability of  $\text{Cu}/\text{Ta}/\text{SiO}_2/\text{Si}$  multilayer structure was studied before and after annealing and the failure mechanism was compared to the uncoated one. It was found that after passivation with  $\text{SiN}_x$  film, the formation of  $\text{Cu}_2\text{O}$  was not observed through out the annealing process.  $\text{Ta}_6\text{O}$  was formed only after  $750^\circ\text{C}$  annealing instead of  $\text{Ta}_2\text{O}_5$ , which was found for the uncoated structure at the same temperature. But the reactions between Cu, Ta and O and formation of  $\text{Cu}_x\text{Ta}_y\text{O}_z$  was fully suppressed in this  $\text{SiN}_x/\text{Cu}/\text{Ta}/\text{SiO}_2/\text{Si}$  multilayer structure. The diffusion barrier found to be failed at  $750^\circ\text{C}$  by out diffusion Ta atoms to the Cu layer and reacted with the dissociated N from  $\text{SiN}_x$  passivation layer and formed TaN. No further reactions were observed to taking place in the structure and no evidence of Cu diffusion through the Ta diffusion layer was found until after annealing at  $850^\circ\text{C}$ . The passivation layer,  $\text{SiN}_x$ , after annealing at  $850^\circ\text{C}$  clearly exhibited ridges and patches and grew as the annealing temperature increased.

#### References

1. S. P. MURARKA, R. J. GUTMAN, A. E. KALOYEROS and W. A. LANFORD, *Thin Solid Films* **236** (1994) 257.
2. Y. SCHACHAM-DIAMAND, A. DEDHIA, D. HOFFSTETTER and W. G. OLDHAM, *J Appl. Phys. Lett.* **60** (1991) 2983.

3. S. P. MURARKA, "Metallization Theory and Practice for VLSI and ULSI" (Butterworth, New York, 1992).
4. JIAN LI and J. W. MAYER, *Mater. Res. Soc. Bull.* **18** (1993) 52.
5. J. LI, P. F. CHAPMAN, Y. SCHACHAN-DIAMAND and J. W. MAYER, "Advanced Metallization of ULSI 1992" (MRS, Pittsburgh, 1993) p. 75.
6. J. LI, J. W. MAYER and E. G. COLGAN, *Appl. Phys.* **70** (1991) 2820.
7. H. ITOW, Y. NAKASAKI, G. MINAMIHABA, K. GUGURO and H. OKANO, *Appl. Phys. Lett.* **63** (1993) 934.
8. J. LI, J. W. MAYER, Y. SCHACHAN-DIAMAND and E. G. COLGAN, *ibid.* **60** (1991) 2983.
9. P. J. DING, W. A. LANFORD, S. HYMES and S. P. MURARKA, *J. Appl. Phys.* **75** (1994) 3627.
10. S. Y. JANG, S. M. LEE and H. K. BAIK, *J. Mater. Sci. Mater. Electron. Soc.* **7** (1991) 271.
11. B. ARCOT, S. P. MURARKA, L. A. CLEVINGER, J. M. E. HARPER and C. CABRAL, in Proceedings of the 9th VLSI Multilevel Interconnection Conference 1992 (unpublished) p. 306.
12. R. NADAN, S. P. MURARKA, A. PANT and C. SHEPARD, *Mater. Res. Soc. Proc.* **260** (1992) 929.
13. L. A. CLEVINGER, N. A. BOHARCZUK, E. HOLLOWAY, J. M. E. HARPER, C. CABRAL, R. G. SCHAD, F. CARDONE and STOLT, *J. App. Phys.* **48** (1993) 1331.
14. R. G. PURSER, J. W. STRANE and J. W. MAYER, in Proceedings of the Materials Reliability in Microelectronics III Symposium (MRS, Pittsburgh, 1993) p. 481.
15. C. A. CHANG, *J. Appl. Phys.* **67** (1990) 6184.
16. S. Q. WANG, I. RAAIJMAKERS, B. J. BURROW, S. SUTHER, S. REDKAR and K. B. KIM, *ibid.* **68** (1990) 5176.
17. K. HOLLOWAY, P. M. FRYER, C. CABRAL, JR., J. M. E. HARPER, P. J. BAILEY and K. H. KELLEHER, *ibid.* **71** (1992) 5433.
18. S. Q. WANG, S. SUTHER, B. J. BURROW and C. HOEFLICH, *ibid.* **73** (1993) 2301.
19. P. J. POKELA, E. KOLAWA, R. P. RUIZ and M. A. NICOLET, *Thin Solid Films* **203** (1991) 259.
20. T. B. MASSALSKI, "Binary Alloy Phase Diagrams," 2nd ed. (ASM/NIST, Metals Park, OH, 1986).
21. K. MAEX and M. V. ROSSUM, "Properties of Metal Silicides," EMIS Data reviews Series No. 14 (INSPEC, London, 1995).
22. S. M. ROSSNAGEL and J. HOPWOOD, *J. Vac. Sci. Technol. B* **12** (1994) 499.
23. T. LAUINGER, J. MOSCHER, A. G. ABERLE and R. HEZEL, *J. Vac. Sci. Technol. A* **16** (1998) 530.
24. JCPDF cards no. Cu (040836),  $\text{Ta}_2\text{N}$  (260985),  $\beta$ -Ta (251280),  $\beta$ - $\text{Si}_3\text{N}_4$  (331160),  $\alpha$ - $\text{Si}_3\text{N}_4$  (410360),  $\text{Ta}_6\text{O}$  (150206) and Si (261481).
25. C. YE, Z. NING, M. SHEN, S. CHENG and Z. GAN, *J. Appl. Phys.* **83** (1998) 5978.
26. Y. K. LEE, K. M. LATT, K. JAEHYEONG, T. OSIPOWICZ and K. LEE, *Materials Science and Engineering B* **68**(2) (1999) 99.
27. H.-J. LEE, K. W. KWON, C. RYU and R. SCINLAIR, *Acta Mater.* **47**(15) (1999) 3965.
28. K. M. LATT, H. S. PARK, S. LI, L. RONG, T. OSIPOWICZ, W. G. ZHU, Y. K. LEE, *J. Mater. Sci.* **37** (2002) 1941.
29. F. L. MARTÍNEZ, A. DEL PRADO, I. MÁRTIL, D. BRAVO and F. J. LÓPEZ, *J. Appl. Phys.* **88** (2000) 2149.
30. S. P. GARG, N. KRISHNAMURTHY, A. AWASTHI and M. VENKATRAMAN, *J. Phase Equilibrium* **17** (1996) 63.
31. J. LI, J. W. MAYER and E. G. COLGAN, *J. Appl. Phys.* **70** (1991) 2820.

Received 8 August 2001  
and accepted 28 May 2002